

A T8.5 Brown Dwarf Member of the Xi Ursae Majoris System

Edward L. Wright¹, M. F. Skrutskie², J. Davy Kirkpatrick³, Christopher R. Gelino³, Roger L. Griffith³, Kenneth A. Marsh³, Tom Jarrett³, M. J. Nelson², H. J. Borish², Gregory Mace¹, Amanda K. Mainzer⁴, Peter R. Eisenhardt⁴, Ian S. McLean¹, John J. Tobin⁵, Michael C. Cushing⁶

ABSTRACT

The Wide-field Infrared Survey Explorer has revealed a T8.5 brown dwarf (WISE J111838.70+312537.9) that exhibits common proper motion with a solar-neighborhood (8 pc) quadruple star system - Xi Ursae Majoris. The angular separation is $8.5'$, and the projected physical separation is ≈ 4000 AU. The sub-solar metallicity and low chromospheric activity of ξ UMa A argue that the system has an age of at least 2 Gyr. The infrared luminosity and color of the brown dwarf suggests the mass of this companion ranges between 28 and 58 M_J for system ages of 2 and 8 Gyr respectively.

Subject headings: brown dwarfs – infrared:stars – solar neighborhood – stars:late-type – stars:low-mass

1. Introduction

The effective temperature and thus spectrum of a brown dwarf evolves with time as it cools as a degenerate object (Kumar 1962). For an isolated brown dwarf, determination of mass and age are intertwined, such that a broad locus of mass and age will be consistent with a single measured effective temperature (Burrows et al. 2003). In rare instances brown dwarfs may reside in close binary systems, resolving this ambiguity with a direct dynamical mass estimation (Konopacky et al. 2010; Cardoso et al. 2009). In the absence of a dynamically measured mass, spectral modeling can significantly constrain a brown dwarf’s mass if there ex-

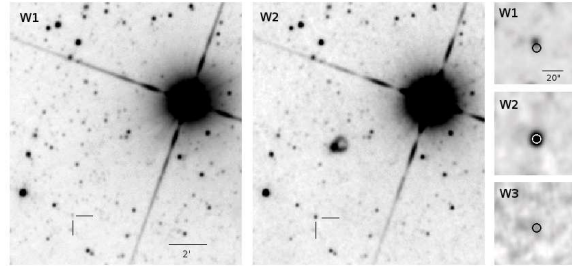


Fig. 1.— WISE All-sky Image Atlas cutouts showing a $10'$ FoV centered halfway between WISE 1118+31 (lower left) and ξ UMa (upper right). The left panel shows W1 ($3.4 \mu\text{m}$), while the right panel shows W2 ($4.6 \mu\text{m}$). The lines point to WISE 1118+31. The odd shape above WISE 1118+31 in the W2 image is a ghost image of ξ UMa. The right-most column shows $1'$ postage stamps of WISE images at 3.4 , 4.6 & $12 \mu\text{m}$.

ists sufficient restriction on the object’s age. Constraints on age and metallicity are available if the brown dwarf is a member of a multiple star system. In this case, the properties of the primary, particularly chromospheric activity and kinematics, provide an indication of age.

The Wide-field Infrared Survey Explorer mis-

¹UCLA Astronomy, PO Box 951547, Los Angeles CA 90095-1547

²Department of Astronomy, University of Virginia, Charlottesville, VA, 22904

³Infrared Processing and Analysis Center, California Institute of Technology, Pasadena CA 91125

⁴Jet Propulsion Laboratory, California Institute of Technology, 4800 Oak Grove Dr., Pasadena, CA, 91109-8001, USA

⁵National Radio Astronomy Observatory, Charlottesville, VA 22903

⁶Department of Physics and Astronomy, MS 111, University of Toledo, 2801 W. Bancroft St., Toledo OH 43606-3328

sion (WISE, Wright et al. 2010) has been a productive engine for the discovery of the coolest brown dwarfs. The WISE W1(3.4 μm) and W2 (4.6 μm) filters are optimally tuned to select the coolest candidates, specifically those with spectra significantly shaped by methane absorption at low effective temperature (Mainzer et al. 2005). To date spectroscopic follow-up of WISE-selected sources has revealed more than 100 ultracool brown dwarfs (Kirkpatrick et al. 2011) including several exceptionally cool Y-dwarfs (Cushing et al. 2011) demonstrating that WISE colors provide for reliable photometric selection of ultra-cool brown dwarf candidates.

WISE J111838.70+312537.9, hereafter WISE 1118+31, easily meets the WISE brown dwarf color selection criterion (Kirkpatrick et al. 2011) with a W1-W2 color of 2.85 compared to a selection threshold of 2.0. Few confusing objects meet these selection restrictions. In addition this source lies 8.5' from one of the nearer stars to the Sun, ξ UMa, prompting an investigation into a possible system membership. This paper reports the spectral characterization of WISE 1118+31 and the analysis of a series of astrometric observations spanning 22 months aimed at determining whether this source exhibits common proper motion with ξ UMa. These observations demonstrate that WISE 1118+31 is a newly found member of this already remarkable multiple star system. The characteristics of the primary system provide an indication of the metallicity and age of the newly discovered ultra-cool brown dwarf constraining the mass of this object.

2. Observations

2.1. WISE

WISE imaged the region of the sky containing WISE 1118+31 on twenty occasions between 21 May 2010 04:20 UT and 25 May 2010 09:39 UT. The WISE All-Sky Catalog reports this source as well detected in W1 and W2, with marginal signal at the position of the W1/2 source in W3 (12 μm) and only an upper limit in W4 (22 μm). Of the twenty apparitions, eighteen were sufficiently separated from a detector edge to permit source extraction. In all eighteen cases the source was detected in W2, producing an combined SNR=34 detection with W2=13.31. Because exceptionally

Table 1: Photometric Observations of WISE 1118+31.

Filter	Vega Magnitude	Instrument
Y	19.18 ± 0.12	FanCam
J	17.792 ± 0.053	WHIRC
J	18.002 ± 0.144	Bigelow
H	18.146 ± 0.060	WHIRC
H	17.686 ± 0.175	Bigelow
Ks	18.746 ± 0.150	WHIRC
W1	16.160 ± 0.071	WISE
ch1	15.603 ± 0.026	IRAC
ch2	13.368 ± 0.018	IRAC
W2	13.308 ± 0.032	WISE
W3	12.359 ± 0.314	WISE
W4	> 8.821	WISE

cool brown dwarfs are considerably fainter in W1, which was optimized to produce a substantial flux difference between W1 and W2, WISE 1118+31 is detected in W1 in only 12 of the 18 opportunities with a combined SNR=15 and W1=16.16, yielding a color of W1-W2=2.85. Figure 1 shows portions of the WISE image atlas covering both WISE 1118+31 and ξ UMa.

2.2. Follow-up Imaging

Multiple epochs of near-infrared imaging provide the astrometric data for WISE 1118+31 needed to confirm common proper motion with ξ UMa. Photometric information from these images is summarized in Table 1 while the astrometric data are listed in Table 2.

2.2.1. Fan Mountain Observatory/FanCam

YJH photometry and astrometry of WISE 1118+31 were obtained at various epochs between 28 Nov 2010 and 15 Mar 2012 with FanCam, a HAWAII-1 based near-infrared imager operating at the University of Virginia's Fan Mountain 31-inch telescope (Kanneganti et al. 2009). The source position was dithered by approximately 10'' between 30 s exposures during total exposures ranging from 60 to 80 minutes. The FanCam field of view (FOV) is 8.7' (0.51''/pixel). The central 7' \times 7' (Figure 2) of the combined, dithered exposures was fully covered, providing several 2MASS stars for photometric and astrometric reference.

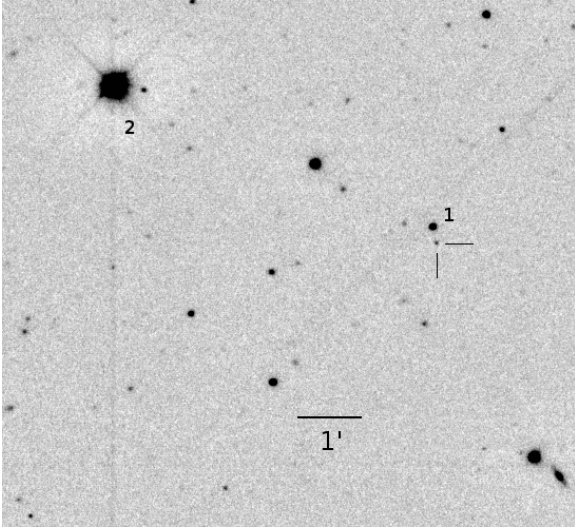


Fig. 2.— Y-band image of the WISE 1118+31 field obtained at Fan Mountain Observatory 15 March 2012 UT. North is up and East is to the left. Perpendicular lines mark the position of WISE 1118+31. Star 1 nearby is the $J=15.94$ star 2MASS J11183876+3125441, while star 2 is 2MASS J11185086+3126520 with $J=10.32$. The faintest detected objects have $Y \approx 20$. The faint diffraction spike entering from the upper left (northwest) is from ξ UMa 8.5' away.

A median sky frame was subtracted from each individual exposure prior to flat fielding with the median background level subsequently restored to the image. YJH aperture photometry was computed using an aperture with a radius of 3 pixels. The zero points for the JH -bands were computed using stars in the FOV with measured 2MASS magnitudes since the JH -band filters in FanCam are based on the 2MASS system. In order to derive the Y -band zero point, we first computed the Y -band magnitudes of stars in the FOV using their 2MASS J and K_s magnitudes and the transformation given by Hamuy et al. (2006). The final uncertainty in the magnitudes include the photon noise from the sky and source, the read noise, and the uncertainty in the zero point. The resulting magnitudes and uncertainties are given in Table 1.

2.2.2. Mount Bigelow/2MASS

The former 2MASS camera on the 1.54m Kuiper Telescope on Mt. Bigelow, Arizona, has three 256×256 -pixel NICMOS3 arrays simultaneously observing in 2MASS J , H , and K_s filters (Milligan et al. 1996). The plate scale for all three arrays is $1.65''/\text{pixel}$, resulting in a $7'$ field of view. Exposures of 10s duration, 216 in all, of WISE 1118+31 were obtained on 20 May 2011 using 6 repeats of a 3×3 box dither pattern, with four consecutive images taken at each of the nine dither positions. The data were reduced using custom IDL routines implementing standard near-infrared flat fielding, background removal, and co-addition techniques. Flat fields in each band were constructed using on-source frames. 2MASS stars provided photometric reference in all three bands.

2.2.3. WIYN/WHIRC

JHK_s broad-band imaging of WISE 1118+31 was obtained on UT 31 Dec 2011 with the WIYN High-Resolution Infrared Camera (WHIRC, Meixner et al. 2010) and the WIYN 3.5-m Observatory. The data quality is excellent: both seeing ($\sim 0.5''$ with $0.1''$ pixel scale) and photometric stability conditions were optimal. For each band, individual frames had exposure times of 120, 120 and 40 seconds, for J , H and K_s , respectively. Using an efficient on-array dither pattern, a total of 7, 9 and 43 frames for J , H and K_s , respectively, were obtained, thus providing a total exposure time of 840, 1080 and 1720 seconds for the J , H and K_s mosaics respectively.

Individual frames were corrected for pupil-ghosts, dark and median sky flat subtracted, normalized by dome flat, and distortion corrected using information from the WHIRC user information guide. Astrometric and photometric solutions using 2MASS standards were then found. The fully reduced frames were combined into a deep mosaic, with outlier (bad pixel) rejection applied using temporal statistics. A final astrometric and flux calibration was then applied to the deep mosaic. The photometric uncertainty (comparing with the 2MASS PSC) was typically better than 5% for each mosaic produced. The achieved spatial resolution was $\sim 0.5 - 0.7''$ for the final mosaics, and the astrometric uncertainty

was $\sim 0.05''$. The target source, WISE 1118+31, was detected in all three bands. Using a $1.1''$ radius circular aperture, the background-subtracted integrated (Vega) magnitudes found are reported in Table 1.

2.2.4. *Spitzer*

The Infrared Array Camera (IRAC) (Fazio et al. 2004) onboard the *Spitzer* Space Telescope employs 256×256 -pixel detector arrays to image a field of view of $5'2 \times 5'2$ ($1''.2 \text{ pixel}^{-1}$). IRAC was used during the warm *Spitzer* mission to obtain deeper photometry in its 3.6 and 4.5 μm channels (hereafter, ch1 and ch2, respectively) than WISE was able to take in its W1 and W2 bands. These observations were made as part of Cycle 7 and Cycle 8 programs 70062 and 80109 (Kirkpatrick, PI). Our standard data acquisition and reduction methodology for IRAC observations is outlined in Kirkpatrick et al. (2011).

2.3. Spectroscopy

2.3.1. *LBT-LUCIFER*

We obtained an *H*- and *K*-band spectrum of WISE 1118+31 on 2012 Dec 12 (UT) using the Large Binocular Telescope (LBT) Near-Infrared Spectroscopic Utility with Camera and Integral Field Unit for Extragalactic Research (LUCIFER, Mandel et al. 2008). A series of twelve 300 s exposures were obtained at different positions along the $4'$ slit to facilitate sky subtraction. The A0 V star HD 97034 was also observed for telluric correction and flux calibration purposes. A series of halogen lamp exposures were also obtained for flat fielding purposes.

The data were reduced using custom Interactive Data Language (IDL) software based on the Spextool data reduction package (Cushing et al. 2004). Pairs of images taken at two different positions along the slit were first subtracted and flat-fielded. The spectra were then extracted and wavelength calibrated using sky emission lines of OH and CH₄. The twelve spectra are combined and then corrected for telluric absorption and flux calibrated using the technique described by Vacca et al. (2003). The final spectrum is shown in Figure 3.

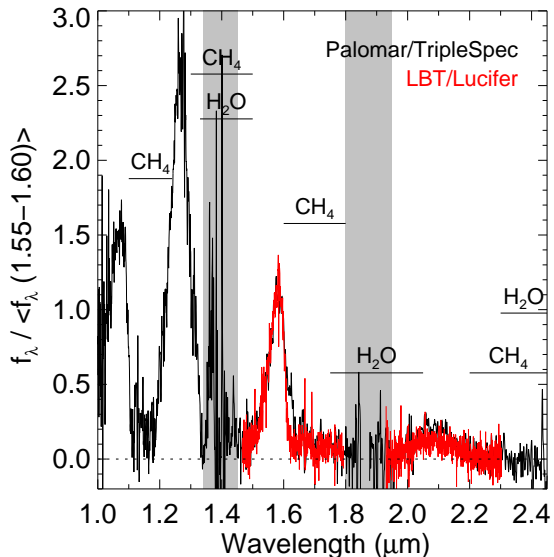


Fig. 3.— Spectrum of WISE 1118+31 obtained with TripleSpec (*black*) and LUCIFER (*red*). Regions of strong telluric absorption are shown in grey. Prominent absorption bands of CH₄ and H₂O are indicated. The agreement between the two spectra is excellent.

2.3.2. *Hale - TripleSpec*

A 1–2.5 μm spectrum of WISE 1118+31 was obtained with the Triple Spectrograph (TripleSpec, Herter et al. 2008) at the 5.08 m Hale Telescope at Palomar Observatory. The 1–2.5 μm range is covered over four cross-dispersed orders which are imaged simultaneously on the 1024×2048 HAWAII-2 array. The $1''$ -wide slit provides a resolving power of $R \approx 2700$. A series of eight, 300 s exposures were obtained at two different positions along the $30''$ -long slit to facilitate sky subtraction. The A0 V star HD 99966 was observed for telluric correction and flux calibration purposes and dome flats were obtained at the start of the night.

The data were reduced using a modified version of the Spextool (Cushing et al. 2004) package; a detailed description of the reduction steps can be found in Kirkpatrick et al. (2011). Briefly, a two-dimensional wavelength solution is derived using sky emission features of OH and CH₄. Spectra are then extracted from pair-subtracted, flat-fielded images. The resulting spectra are com-

binned and corrected for telluric absorption and flux calibrated on an order-by-order basis. Finally, the spectra from each order are stitched together to form a complete 1–2.5 μm spectrum. The spectrum was then flux calibrated as described in Rayner et al. (2009) using the photometry in Table 1. The final spectrum is shown in Figure 3.

3. Discussion

3.1. Properties of ξ UMa

ξ Ursae Majoris¹ is a complex stellar system with at least 4, and possibly 5 components (Mason et al. 1995) known prior to the discovery of WISE 1118+31. Visible to the unaided eye a short distance from the Big Dipper, this telescopic double star was the among the first to be recognized as a gravitationally bound binary system (Herschel 1804). Given the 59.84 year period of the visual pair it was not until 23 years later that Struve (1827) calculated a formal orbit. Subsequently both components of the visual pair with $a = 2.530''$ were found to be spectroscopic binaries. These binaries have periods of 669.1 for the Aa system and 3.9805 days for the Bb system, parameters taken from Heintz (1967). Heintz (1967) also found $M_A = 0.83 M_\odot$, its companion in the 669 day orbit had mass $M_a = 0.31 M_\odot$, and the combined mass of the 4 day binary was $M_B + M_b = 0.91 M_\odot$, with $M_b \sin i = 0.04 M_\odot$. Finally Heintz (1967) gives a distance of 7.7 ± 0.2 pc (parallax of $0.130'' \pm 0.002''$) from comparing the visual and spectroscopic orbits of the system. The speckle data of Mason et al. (1995) only changed a by 0.24% to $a = 2.536''$, so the uncertainty in the distance is dominated by the radial velocity amplitudes. Griffin (1998) gave new velocity amplitudes, $K_A = 4.85 \pm 0.14$ km/sec and $K_B = 4.33 \pm 0.09$ km/sec leading to a new parallax estimate of $0.126'' \pm 0.0023''$ but the mass ratio is reversed with the brighter A component being less massive than the Bb system casting doubts on the precision of the results. A low inclination for the 4 day binary’s orbit could reconcile these results by putting more of the total Bb mass into B’s unseen companion.

¹also Alula Australis, HR 4374/5, Gl 423, HD 98230/1

3.1.1. Spectral Types and Metallicities of the Primaries

Cayrel de Strobel et al. (1994) used high resolution spectroscopy to find effective temperatures and gravities of 5950 ± 30 K, $\log g = 4.3 \pm 0.2$ for ξ UMa A; and 5650 ± 50 K, $\log g = 4.5 \pm 0.2$ for B. These temperatures and gravities are consistent with spectral types of F8.5V and G2V assigned to ξ UMa A and B by Keenan & McNeil (1989).

Cayrel de Strobel et al. (1994) found that both stars had slightly sub-solar iron abundances, $[\text{Fe}/\text{H}] = -0.32 \pm 0.05$ dex. They found that the luminosities (for parallax $0.130''$) and effective temperatures were consistent within the errors with the masses derived by Heintz (1967) for a 5 Gyr isochrone calculated with sub-solar abundance.

3.1.2. Parallax and Proper Motion

Karataş et al. (2004) gives a parallax of $0.1132'' \pm 0.0046''$, but ξ UMa was not included in the recalculation of the Hipparcos results by van Leeuwen (2007), possibly due to complications produced by the motion of the visual AB binary and astrometric wobble of Aa. However Söderhjelm (1999) re-analyzed the Hipparcos data combined with other data for visual binaries and gives $0.1197'' \pm 0.0008''$ for the parallax of ξ UMa. The weighted mean of $0.126'' \pm 0.0023''$ from the ratio of the visual orbit semi-major axis to the spectroscopic semi-major axis and $0.1197'' \pm 0.0008''$ is $0.1206'' \pm 0.00074''$ but $\chi^2 = 8.6$ for 1 degree of freedom in the fit for the mean, so we inflate the errors by a factor of $\sqrt{8.6}$ and adopt $0.1206'' \pm 0.0022''$ for the parallax. Bakos et al. (2002) give a proper motion of $0.75''/\text{yr}$ in position angle 217.49° , based on a 29 year interval. These values resolve into $-0.456''/\text{yr}$ and $-0.595''/\text{yr}$ which we adopt.

3.1.3. Chromospheric Activity and Age

Cayrel de Strobel et al. (1994) see chromospheric calcium emission lines for ξ UMa B but not for ξ UMa A. They propose that the short 4 day period orbit of the Bb system is driving the chromospheric activity in B. From the lack of emission in A, Cayrel de Strobel et al. (1994) conclude that ξ UMa is older than stars in the cluster NGC 752, which has an age of 2 Gyr. Ball et al. (2005) report X-ray observations of ξ UMa which show

that all of the observed X-ray emission is coming from the 4 day period binary Bb. X-ray flux from component A is more than 2 orders of magnitude fainter, implying $\log L_X < 27.5$. Since component A is close to solar luminosity, the ratio of X-ray to bolometric flux is $R_X = \log(L_X/L_{bol}) < -6$ which gives an age greater than 4 Gyr using Equation(A3) in Mamajek & Hillenbrand (2008). The low space velocity reported by Karataş et al. (2004) implies that ξ UMa is a member of the thin disk, so ages much greater than 8 Gyr are unlikely.

3.2. Astrometry and System Membership

Astrometric information was extracted from the observed images at the various epochs using the standard maximum likelihood technique in which a point spread function (PSF) was fit to each source profile. The positional uncertainties were estimated using an error model which includes the effects of instrumental and sky background noise and PSF uncertainty. The PSF and its associated uncertainty map were estimated for each image individually using a set of bright stars in the field. In order to minimize systematic effects, our astrometry was based on relative positions, using as a reference the nearby star 2MASS J11183876+3125441 at a separation of approximately $6.5''$. This is sufficiently close that systematic errors due to such effects as focal-plane distortion, and plate scale and rotation errors cancel out in the relative position to an accuracy much greater than the random estimation errors. We do, however, assume that the proper motion and parallax of the reference star are negligible compared to those of WISE 1118+31. In support of this assumption, we find no significant difference in relative motion of WISE 1118+31 when the differential astrometry is repeated using more distant 2MASS reference stars, at separations of $69''$ and $105''$. The astrometric estimation procedure is discussed in more detail by Marsh et al. (2012).

These values were converted into α and δ in degrees for input to a parallax and proper motion code that handles both Earth-based and Spitzer observations. Table 2 gives these values. Table 3 gives the output from the code for three different sets of free parameters. In one case the proper motion and parallax were forced to zero. In the second case they were forced to match ξ UMa. In the final case the proper motion and parallax were

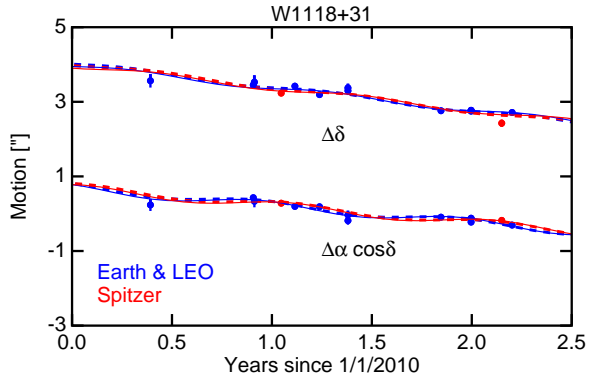


Fig. 4.— Astrometric data and fits for WISE 1118+31. The blue curves and points are for ground-based or Low Earth Orbit observatories, while the red curves and points are for Spitzer. The bold dashed lines show the fit with proper motion and parallax as free parameters, while the lighter solid curves show the fit forced to match ξ UMa. These fits are essentially indistinguishable.

left as free parameters.

The astrometric fits for WISE 1118+31 are a very good match to the motion of ξ UMa. The $\Delta\chi^2 = 547.6$ between the best fit and a fit with a fixed position shows that the motion of WISE 1118+31 has been detected with a SNR of 23, while the $\Delta\chi^2 = 2.25$ for 3 extra degrees of freedom between the best fit and a fit forced to match the proper motion and parallax of ξ UMa is perfectly consistent with WISE 1118+31 being a bound member of the ξ UMa system. Figure 4 shows two fits: one forced to match ξ UMa and one with the proper motion and parallax as free parameters.

3.3. Spectral Classification

As shown in Figure 3, the spectrum of WISE 1118+31 exhibits deep absorption bands of CH_4 and H_2O indicative of T dwarfs. We derive a more precise spectral type using the spectral classification schemes of Burgasser et al. (2006) and the extension to this system by Cushing et al. (2011) whereby UGPS J072227.51-054031.2 (hereafter UGPS 0722-05, Lucas et al. 2010) is defined as the T9 spectral standard and WISE 1738+2732 is defined as the Y0 spectral standard. As shown in Figure 5, WISE 1118+31 has a spectral type

Table 2: Astrometric Observations of WISE 1118+31.

Date	R.A. [°]	$\cos \delta \sigma(\alpha)$ ["]	Dec [°]	$\sigma(\delta)$ ["]	Observatory	Band
2010.39	169.661109	0.162	31.427016	0.182	WISE	W2
2010.91	169.661172	0.050	31.426985	0.050	FanMt	Y
2010.91	169.661141	0.162	31.427006	0.184	WISE	W2
2011.05	169.661124	0.074	31.426924	0.068	Spitzer	ch2
2011.12	169.661096	0.050	31.426976	0.050	FanMt	J
2011.24	169.661093	0.050	31.426913	0.050	FanMt	J
2011.38	169.660972	0.110	31.426963	0.113	MtBglw	J
2011.38	169.661021	0.116	31.426942	0.116	MtBglw	H
2011.85	169.661002	0.050	31.426793	0.050	FanMt	J
2012.00	169.660993	0.050	31.426790	0.050	WIYN	J
2012.00	169.660989	0.050	31.426796	0.050	WIYN	H
2012.00	169.660959	0.050	31.426795	0.050	WIYN	K
2012.15	169.660974	0.079	31.426700	0.093	Spitzer	ch2
2012.20	169.660933	0.050	31.426780	0.050	FanMt	Y

Table 3: Astrometric Fits for WISE 1118+31.

Type	χ^2	#df	$\cos \delta d\alpha/dt$ ["/yr]	$d\delta/dt$ ["/yr]	ϖ ["]
Fixed	580.733	26	0	0	0
Forced to ξ UMa	35.336	26	-0.456	-0.595	0.1206
Free	33.089	23	-0.478 ± 0.034	-0.633 ± 0.034	0.104 ± 0.025

of T8.5 based on the width of the J-band peak at 1.27 μm .

3.4. The View from the Neighborhood of WISE 1118+31

With a projected separation of 4100 AU from the four main components of the ξ UMa system, WISE 1118+31 has a distant but interesting perspective. The two binaries that form the 2'' visual pair as seen from the Earth are separated by 20 AU, or by an angular scale of 15' from the distant perspective of WISE 1118+31. At that distance the A and B components would each shine with an apparent visual magnitude of -9, one hundred times brighter than Venus in the skies of Earth.

Given the complexity of the ξ UMa system, it is reasonable to speculate that WISE 1118+31 could be an ejected component that was once more closely bound to the system, possibly explaining the tight binary ξ UMa Bab. Given an orbital period of order 10^5 years, the orbital eccentricity of WISE 1118+31 will ultimately be measurable. With an apparent orbital radius of 8.5' this orbital

motion will amount to tens of milliarcseconds per year relative to the primary system. Characterizing this motion, specifically the differential proper motion between WISE 1118+31 and its primary, is tractable given modern infrared and visual astrometric capability, and certainly will be accomplished with the passage of time.

4. Conclusions

Alula Australis (ξ UMa), a solar neighborhood visual binary where each component is itself a spectroscopic binary, possesses an ultra-cool brown dwarf (T8.5) companion at a projected separation of 4100 AU. For our adopted parallax the absolute magnitude is $M_{W2} = W2 + 5 \log(10\varpi) = 13.715 \pm 0.051$. This agrees very well with the M_{W2} vs. type relation in Kirkpatrick et al. (2011) which gives $M_{W2} = 13.71 \pm 0.21$ for a spectral type of $T8.5 \pm 0.5$. The low chromospheric activity of the A component and a system metallicity of $[\text{Fe}/\text{H}] = -0.35$ suggest the system is of approximately solar age. Modified Burrows et al. (2003) models with a flux suppression of $f = 0.22$ (Wright et al. 2010),

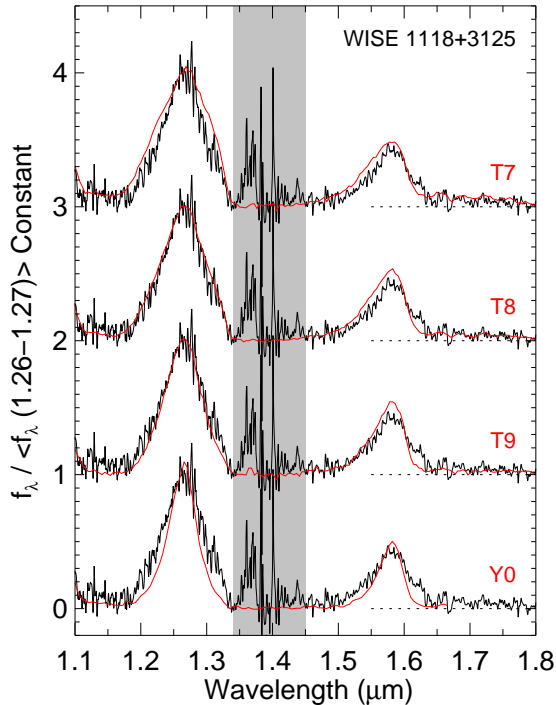


Fig. 5.— Sequence of spectral standards from T7 to Y0 (red) along with the spectrum WISE 1118+31 (black). The spectral standards are 2MASS 0727+1710 (T7, Burgasser et al. 2006) and 2MASS 0415-0935 (T8, Burgasser et al. 2006), UGPS 0722-05 (T9, Cushing et al. 2011), and WISE 1738+2732 (Y0, Cushing et al. 2011). The spectrum of WISE 1118+3125 has been smoothed to a resolving power of $\lambda/d\lambda = 1000$ for display purposes. Spectra are normalized to unity over the 1.26-1.27 μm wavelength range and offset for clarity (dotted lines). Regions of high telluric absorption are shown in grey. WISE 1118+3125 is classified as T8.5.

which match both the W1-W2 color and M_{W2} of WISE 1118+31 constrain the mass of this distant companion to be between 28 and 58 M_J for ages between 2 and 8 Gyr. Thus this system provides a very accurate absolute magnitude for a T8.5 brown dwarf, but both the age of the system and the mass of the brown dwarf are uncertain due to the difficulty of determining the age of a star in the middle of its main sequence lifetime.

This publication makes use of data products from the Wide-field Infrared Survey Explorer, which is a joint project of the University of California, Los Angeles, and the Jet Propulsion Laboratory/California Institute of Technology, funded by the National Aeronautics and Space Administration.

Facilities: WISE, Fan Mountain/FanCam, LBT/LUCIFER, Palomar/TripleSpec, Mt. Bigelow/Kuiper-2MASS, WIYN/WIRC.

REFERENCES

- Bakos, G. Á., Sahu, K. C., & Németh, P. 2002, *ApJS*, 141, 187
- Ball, B., Drake, J. J., Lin, L., Kashyap, V., Laming, J. M., & García-Alvarez, D. 2005, *ApJ*, 634, 1336
- Burgasser, A. J., Geballe, T. R., Leggett, S. K., Kirkpatrick, J. D., & Golimowski, D. A. 2006, *ApJ*, 637, 1067
- Burrows, A., Sudarsky, D., & Lunine, J. I. 2003, *ApJ*, 596, 587
- Cardoso, C. V., McCaughrean, M. J., King, R. R., Close, L. M., Scholz, R.-D., Lenzen, R., Brandner, W., Lodieu, N., & Zinnecker, H. 2009, in *American Institute of Physics Conference Series*, Vol. 1094, American Institute of Physics Conference Series, ed. E. Stempels, 509–512
- Cayrel de Strobel, G., Cayrel, R., Friel, E., Zahn, J.-P., & Bentolila, C. 1994, *A&A*, 291, 505
- Cushing, M. C., et al. 2011, *ApJ*, 743, 50
- Cushing, M. C., Vacca, W. D., & Rayner, J. T. 2004, *PASP*, 116, 362
- Fazio, G. G., et al. 2004, *ApJS*, 154, 10

- Griffin, R. F. 1998, *The Observatory*, 118, 273
- Hamuy, M., et al. 2006, *PASP*, 118, 2
- Heintz, W. D. 1967, *Astronomische Nachrichten*, 289, 269
- Herschel, W. 1804, *Royal Society of London Philosophical Transactions Series I*, 94, 353
- Herter, T. L., et al. 2008, in *Society of Photo-Optical Instrumentation Engineers (SPIE) Conference Series*, Vol. 7014, *Society of Photo-Optical Instrumentation Engineers (SPIE) Conference Series*
- Kanneganti, S., Park, C., Skrutskie, M. F., Wilson, J. C., Nelson, M. J., Smith, A. W., & Lam, C. R. 2009, *PASP*, 121, 885
- Karataş, Y., Bilir, S., Eker, Z., & Demircan, O. 2004, *MNRAS*, 349, 1069
- Keenan, P. C. & McNeil, R. C. 1989, *ApJS*, 71, 245
- Kirkpatrick, J. D., et al. 2011, *ApJS*, 197, 19
- Konopacky, Q. M., Ghez, A. M., Barman, T. S., Rice, E. L., Bailey, III, J. I., White, R. J., McLean, I. S., & Duchêne, G. 2010, *ApJ*, 711, 1087
- Kumar, S. S. 1962, *AJ*, 67, 579
- Lucas, P. W., et al. 2010, *MNRAS*, 408, L56
- Mainzer, A. K., Eisenhardt, P., Wright, E. L., Liu, F.-C., Irace, W., Heinrichsen, I., Cutri, R., & Duval, V. 2005, in *Presented at the Society of Photo-Optical Instrumentation Engineers (SPIE) Conference*, Vol. 5899, *UV/Optical/IR Space Telescopes: Innovative Technologies and Concepts II*. Edited by MacEwen, Howard A. *Proceedings of the SPIE*, Volume 5899, pp. 262-273 (2005)., ed. H. A. MacEwen, 262–273
- Mamajek, E. E. & Hillenbrand, L. A. 2008, *ApJ*, 687, 1264
- Mandel, H., et al. 2008, in *Society of Photo-Optical Instrumentation Engineers (SPIE) Conference Series*, Vol. 7014, *Society of Photo-Optical Instrumentation Engineers (SPIE) Conference Series*
- Marsh, K., et al. 2012, in preparation
- Mason, B. D., McAlister, H. A., Hartkopf, W. I., & Shara, M. M. 1995, *AJ*, 109, 332
- Meixner, M., et al. 2010, *PASP*, 122, 451
- Rayner, J. T., Cushing, M. C., & Vacca, W. D. 2009, *ApJS*, 185, 289
- Söderhjelm, S. 1999, *A&A*, 341, 121
- Struve, F. G. W. 1827, *Catalogus novus stellarum duplicium et multiplicium (Dorpati [Tartu] : typis J. C. Schuenmanni)*
- Vacca, W. D., Cushing, M. C., & Rayner, J. T. 2003, *PASP*, 115, 389
- van Leeuwen, F., ed. 2007, *Astrophysics and Space Science Library*, Vol. 350, *Hipparcos, the New Reduction of the Raw Data*
- Wright, E. L., et al. 2010, *AJ*, 140, 1868